Published in final edited form as:
*Exp Cell Res*. 2011 October 15; 317(17): 2522–2535. doi:10.1016/j.yexcr.2011.08.006.

# Mammalian ChlR1 has a role in heterochromatin organization

**Akira Inoue**[a], **Judith Hyle**[a], **Mark S. Lechner**[b], and **Jill M. Lahti**[a,c,*]

[a]Department of Tumor Cell Biology, St. Jude Children's Research Hospital, Memphis, TN, USA

[b]Faculty of Health Sciences, Simon Fraser University, Burnaby, BC, Canada

[c]Department of Molecular Sciences, University of Tennessee Health Science Center, Memphis, TN, USA

## Abstract

The ChlR1 DNA helicase, encoded by *DDX11* gene, which is responsible for Warsaw breakage syndrome (WABS), has a role in sister-chromatid cohesion. In this study, we show that human ChlR1 deficient cells exhibit abnormal heterochromatin organization. While constitutive heterochromatin is discretely localized at perinuclear and perinucleolar regions in control HeLa cells, ChlR1-depleted cells showed dispersed localization of constitutive heterochromatin accompanied by disrupted centromere clustering. Cells isolated from $Ddx11^{-/-}$ embryos also exhibited diffuse localization of centromeres and heterochromatin foci. Similar abnormalities were found in HeLa cells depleted of combinations of HP1α and HP1β. Immunofluorescence and chromatin immunoprecipitation showed a decreased level of HP1α at pericentric regions in ChlR1-depleted cells. Trimethyl-histone H3 at lysine 9 (H3K9-me3) was also modestly decreased at pericentric sequences. The abnormality in pericentric heterochromatin was further supported by decreased DNA methylation within major satellite repeats of $Ddx11^{-/-}$ embryos. Furthermore, micrococcal nuclease (MNase) assay revealed a decreased chromatin density at the telomeres. These data suggest that in addition to a role in sister-chromatid cohesion, ChlR1 is also involved in the proper formation of heterochromatin, which in turn contributes to global nuclear organization and pleiotrophic effects.

### Keywords

ChlR1; *DDX11*; HP1; heterochromatin; H3K9-me; DNA methylation

## Introduction

Human ChlR1 and its closely related relative ChlR2 are DNA helicases belonging to the FANCJ helicase family [1,2]. These helicases are encoded by the *DDX11* and *DDX12* genes, respectively, which are located on the short arm of chromosome 12 [3]. Mutants of the yeast ortholog, *CHL1*, exhibit chromosome missegregation at high frequencies [4], due to a defect in sister-chromatid cohesion [5,6]. Mammalian ChlR1-deficient cells have similar defects in sister-chromatid cohesion [7,8]. A recent genetic study revealed that *DDX11* is the gene



*Correspondence author at: Department of Tumor Cell Biology, St. Jude Children's Research Hospital, 262 Danny Thomas Place, Memphis, TN 38105, USA. Tel: +1 901 595 3501. Fax: +1 901-595 2381. jill.lahti@stjude.org (J.M. Lahti).

responsible for a genetic disease, Warsaw breakage syndrome (WABS). The major clinical symptoms of WABS are pre- and postnatal developmental abnormalities, including facial anomalies and mental retardation, as well as cohesion defects [9]. Similar defects in development and cohesion are seen in patients with other cohesinopathies, which are caused by mutations of either cohesin genes or genes required for cohesion [10]. These data suggest that the genes responsible for cohesinopathy might have additional functions in processes other than sister-chromatid cohesion. Based on the fact that cohesins collaborate with CTCF [11], a highly conserved zinc finger protein that is involved in diverse regulatory functions through the global organization of chromatin architecture [12], these defects might include aberrant patterns of gene expression.

Yeast *chl1* mutants exhibit a cohesion defect. However, these mutants show additional phenotypes including increased ribosomal DNA recombination rates and transcriptional gene silencing [13]. Although budding yeast does not have the same heterochromatin organization as higher eukaryotes, these processes in higher eukaryotes involve heterochromatin. It is thus suggested that CHL1 may be involved in heterochromatin-like functions. Indeed, the role of yeast CHL1 in transcriptional silencing depends on the presence of SIR2 [13], a protein recognized to function in heterochromatin-like events in budding yeast [14]. These data led us to postulate that mammalian ChlR1 and ChlR2 might have a role in heterochromatin-related events.

Heterochromatin is found in the region of chromosomes that remain highly condensed and transcriptionally silenced [15]. Studies on epigenetic modifications of chromatin, especially covalent modifications of core histones, have revealed that histone H3 is methylated at lysine 9 (H3K9-me) in these regions by the specific methyltransferases, SUV39H1 and SUV39H2 [16]. H3K9-me in turn recruits heterochromatin protein 1 (HP1) through binding to the chromo domain (CD) of HP1 [17,18]. The chromo-shadow domain (CSD) of HP1 also binds to various other proteins such as SUV39H1, Kap-1/Tif1β, BRG1, ATRX, and lamin B receptor [19] through a PXVXL/I motif which is required for the binding to CSD [20]. Thus, HP1 is believed to function as a platform for various effecter proteins involved in heterochromatin formation such as DNA methyltransferases [21,22]. DNA methyltransferases function in methylating cytosine nucleotides in the context of CpG sequences. CpG methylation is another hallmark of heterochromatin which contributes to the transcriptionally silent nature of heterochromatin [20]. Abnormalities in the epigenetic marking on the genome can result in an aberrant pattern of gene expression.

In this study, we show heterochromatin-related defects in ChlR1-deficient mammalian cells that are similar to those found in cells depleted of both HP1α and HP1β. In addition, studies using immunofluorescence (IF) and chromatin immunoprecipitation (ChIP) revealed an impaired localization of HP1α at the pericentric regions in the absence of ChlR1. We also found there was a decrease in telomeric chromatin density in these cells. Furthermore, mouse embryos lacking *Ddx11* showed impaired levels of DNA methylation at the major satellite repeats. These data suggest that ChlR1 might have a role in heterochromatin formation and function in mammalian cells.

## Materials and Methods

### Antibodies

Antibodies used for immunofluorescence were anti-HP1α (mouse MAB3584, Millipore), anti-HP1β (mouse MAB3448, Millipore), anti-HP1γ (mouse MAB3450, Millipore), anti-trimethyl-histone H3 at lysine 9 (H3K9-me3) (rabbit CS200604, Millipore), anti-phospho-histone H3 at serine 10 (P-H3S10) (rabbit 07–523, Millipore) and anti-centromere autoimmune (ACA) serum (human, Antibodies Incorporated). Antibodies used for

immunoblot were anti-HP1α (mouse clone 15.19s2, Millipore), anti-HP1β (mouse MAB3448), anti-ChlR1 (rabbit Hel1) [1], and anti-actin (goat sc-1615, Santa Cruz Biotechnologies). Antibodies used for chromatin immunoprecipitation (ChIP) were anti-HP1α (rabbit #2090, S. Smale, UCLA) and anti-H3K9-me3 (CS200604).

## Cell culture and immunofluorescence

HeLa cells and HeLa cells stably expressing EGFP-histone H2B [23] were used in this study. For immunofluorescence, cells grown on slides or coverslips were fixed with 4% paraformaldehyde (PFA) in PBS for 12 min at room temperature and permeabilized with 0.2% Triton X-100 in phosphate buffer (150 mM, pH7.4) for 15 min. The preparations were then blocked with 3% fetal bovine serum (FBS) in PBS for 15 min at room temperature. Primary antibodies diluted in the blocking solution were applied and incubated for 1 h at 37 C in a humidified chamber. After washing with PBS, secondary antibodies were applied to stain the cells. The slides or coverslips were mounted with Vectashield (Vector Laboratories) containing 0.75 μg/ml DAPI. Fluorescence microscopy was done on E800 microscope (Nikon) with a DXM1120 digital camera (Nikon). For some preparations confocal microscopy was done on C1Si microscope (Nikon) with a Cascade 512B photomultiplier (Photometrics). Images were processed using EZC1 (Nikon) and Photoshop 7 (Adobe).

In some experiments, a pre-extraction procedure was performed to remove proteins loosely associated with chromatin according to the method described previously [24]. Cells grown on coverslips were washed first with PBS+ which contains 0.5 mM $MgCl_2$ and 0.5 mM $CaCl_2$ and then with cytoskeleton (CSK) buffer (10 mM Pipes-KOH, pH 7.0, 100 mM NaCl, 300 mM sucrose and 3 mM $MgCl_2$) [25]. Cells were incubated in CSK buffer supplemented with 0.5% Triton X-100, 0.5 mM PMSF (Sigma), and 10 mg/ml leupeptin (Sigma) for 5 min on ice. After two washes with CSK buffer, the cells were fixed in 4% paraformaldehyde for 15 min at room temperature. The coverslips were served for immunostaining as described above. Confocal microscopy and image processing were carried out as described above. In some studies, cells were treated with the aurora-kinase inhibitor, ZM447439 (AstraZeneca). For these studies ZM447439 was added to the culture at a concentration of 2 μM for 1 hr prior to the fixation and immunostained as described above. In addition, unfixed HeLa cells expressing EGFP-histone-H2B chromatin density were also examined using a Zeiss AxioObserver microscope (Marianas, Carl Zeiss). Quantitation of fluorescence of pericentric HP1α signals was performed using the NIS-Elements software (Nikon) on confocal images acquired with a C1Si microscope.

## siRNA experiments

Depletion of ChlR1 and ChlR2 was performed as previously described [8]. Briefly, a plasmid expressing #4 or #5 shRNA was electroporated twice into HeLa cells at an interval of 24 hrs. For the chromatin immunoprecipitation experiment, a clone permanently depleted of ChlR proteins (clone 5.5) was used. This was established by infecting HeLa cells with pantropic retrovirus (pSuper-Retro-Puro) expressing #5 shRNA [8] and selected with puromycin. A control clone (C1) was also obtained. For depletion of HP1α, pSuper-Retro-Puro expressing shRNAs targeting the indicated mRNA was used to infect HeLa cells or HeLa cells expressing EGFP-H2B. Clones were obtained by puromycin selection. For depletion of HP1β, pSuper-Retro-Puro targeting HP1β was transiently transfected according to the method previously described [8]. The target sequences of 3 HP1 isoforms described in a previous report were used [26] and 5′-GGAGCACAATACTTGGGAA-3′ (nt; 272–290, NM_012117) was used to target HP1α.

### Chromatin immunoprecipitation (ChIP)

ChIP was performed as described previously [27,28] with modifications as follows: Nuclei isolated by Dignam's method were crosslinked with 1% formaldehyde for 3 min at room temperature. Chromatin fragmentation was done using micrococcal nuclease (MNase) (50 U/ml, Worthington) in nuclear digestion buffer (15 mM HEPES (pH7.5), 60 mM KCl, 15 mM NaCl, 0.34 mM sucrose, 1 mM DTT, and 0.5 mM spermidine) for 8 min at room temperature. Digested nuclei were sonicated briefly and centrifuged at 3,800g for 5 min at 4C. The supernatant was collected and precleared with protein A beads (Pierce) at 4C for 1 hr. After pelleting the beads the remaining supernatant was used for immunoprecipitation. Four μg of antibody was added to the supernatant containing 300 μg of protein, and incubated at 4C overnight in the lysis buffer (25 mM Tris-Cl (pH7.5), 150 mM NaCl, 5 mM EDTA, 1% Triton X-100, 0.1% SDS, and 0.5% sodium deoxycholate) in the total volume of 1 ml. Protein-A beads were then added and the samples were rocked for 1 hr at 4C. The beads were washed with a series of buffers as follows, lysis buffer, RIPA buffer, high-salt buffer, LiCl buffer, and TE buffer [29]. DNA was eluted from the beads in the elution buffer (2% SDS, 0.1 M $NaHCO_3$, and 10 mM DTT) and DNA-protein crosslink was released by incubating the eluate at 60C overnight. After digestion with proteinase K for 2 hr at 55C, DNA was purified from the mixture using the ChIP DNA Clean & Concentrator Kit (Zymo Research). To quantitate the precipitated DNA, dot blots were hybridized with $^{32}$P-labeled β-satellite probe (p21β2) [30], telomere probe (pSP73.Sty11) [31], and *Alu* probe [30]. The intensity of hybridization signals was measured by a phosphoimager (Molecular Dynamics). Percent recovery rate for each genomic region was calculated using the formula:

Recovery (%) = 100 × (R5.5 [H3K9-me3 or HP1α] − R5.5 [preimmune])/(R1 [H3K9-me3 or HP1α] − R1 [preimmune]), where R is the radioactive count from the dot blot using the specific antibody for H3K9-me3, HP1α, or the preimmune serum as indicated. R5.5 is the count obtained from the ChlR-depleted HeLa clone 5.5. R1 is the count obtained from the control HeLa clone C1.

### Micrococcal nuclease (MNase) assay

MNase assay was performed as described previously [32]. Briefly, cells in a culture dish were permeabilized with 0.01% L-α-lysophosphatidylcholine (Sigma) in 150 mM sucrose, 80 mM KCl, 35 mM HEPES (pH 7.4), 5 mM $K_2HPO_4$, 5 mM $Mg_2Cl$, and 0.5 mM $CaCl_2$ for 90 s, followed by digestion with 2 U/ml MNase in 20 mM sucrose, 50 mM Tris (pH 7.5), 50 mM NaCl, and 2 mM $CaCl_2$ at room temperature. The reactions were stopped at the indicated time points by adding 20 mM EDTA and DNA was subjected to 0.8% agarose gel electrophoresis. The pattern of DNA fragmentation was visualized by EtBr staining and Southern hybridization using radioactive probes used in ChIP.

### Analysis of DNA methylation

Whole E9.5 embryos or ES cells were digested with proteinase K and DNA was isolated from the aqueous phase after phenol/chloroform/isoamylalcohol (25:24:1) extraction. Isopropanol was then added to the aqueous phase and DNA was recovered by spooling. Two μg DNA was used for endonuclease digestion with *Msp*I or *Hpa*II. Digests were separated in 0.8 % agarose gel electrophoresis followed by Southern blotting onto Hybond-N membranes. DNA was cross-linked by Stratalinker (Stratagene) at 1,200 J/$m^2$. DNA bands were detected by [$^{32}$P]-labeled mouse major satellite or minor satellite probe, which were retrieved by PCR from genomic DNA. Signals were visualized by autoradiography.

## Results

### Aberrant localization of heterochromatin foci and centromeres in cells cultured from Ddx11$^{-/-}$ embryos

Previously we analyzed sister-chromatid cohesion in cells from embryos lacking ChlR1, a protein encoded by the single mouse gene *Ddx11* [8]. Because *Ddx11*$^{-/-}$ results in embryonic lethality at E10.5 [8], cells were cultured from trypsinized E9.5 *Ddx11* null and wild-type embryos and stained with DAPI for some of these experiments. While analyzing the chromosomes from these cells we noticed differences in the DAPI staining pattern of interphase nuclei from *Ddx11*$^{-/-}$ and wild-type embryos. A normal mouse nucleus exhibits variations in the intensity of DAPI staining within a nucleus due to several large clusters of pericentric heterochromatin in the nucleoplasm [33]. When *Ddx11*$^{+/+}$ cells were stained with DAPI, the pericentric heterochromatin clusters were clearly observed as DAPI-dense foci as expected (Fig. 1A panel a). Contrary to this, cells isolated from *Ddx11*$^{-/-}$ embryos exhibited more diffuse DAPI staining (Fig. 1A panel d). To verify that these DAPI-dense regions contained pericentric heterochromatin we stained the cells from the *Ddx11* null and control embryos with an autoimmune serum that recognizes centromeric proteins (ACA). The centromeric signals were visible in the DAPI dense regions and appeared as distinct strongly stained spots in the control cells (Fig. 1A panel b). The number of signals was much fewer than the total number of mouse chromosomes (=40), which suggests that centromeres of several chromosomes were clustered in a single signal. In contrast, more than the expected number of weakly stained centromere signals was observed in the *Ddx11* null cells (Fig. 1A panel e). The increase in centromeric signals most likely reflects the fact that a substantial fraction (~20%) of *Ddx11*$^{-/-}$ cells, including the cell shown in Fig. 1A, was polyploid due to aberrant mitosis caused by the cohesion defect [7,8,34]. However, because these centromere signals were much weaker than those in control cells, these data also implied that the centromere clustering is disrupted in *Ddx11*$^{-/-}$ cells. Taken together these data suggest that ChlR1 may be required for the proper localization and possibly formation of heterochromatin.

### Human ChlR-deficient cells have dispersed heterochromatin regions with disrupted centromere clustering

To determine whether loss of human ChlR1 and 2 also alters the distribution of heterochromatin in human cells, HeLa cells were depleted of both ChlR1 and ChlR2, which will be collectively called ChlR hereafter in this report, by transfection with ChlR specific shRNA-expressing plasmids that target regions of complete homology in the mRNAs encoded by the two genes. Two plasmids expressing #4 and #5 shRNA efficiently depleted ChlR proteins in HeLa cells [8] (Fig. 1B). Although the global localization pattern of heterochromatin is quite different in human and mouse cells and human heterochromatin is less obvious microscopically [33], we still noticed differences in the relative location of the DAPI rich regions in the control and ChlR-deficient cells (Fig. 1C panels *b* and *d*). To confirm this observation we also stained the cells with antibodies recognizing HP1α, a protein which is known to localize to heterochromatin-rich regions [33,35]. Control cells clearly showed heterochromatin regions in perinuclear and perinucleolar areas both by anti-HP1α staining and DAPI staining (Fig. 1C panels *a* and *b*). To determine whether these regions contained pericentric heterochromatin we stained the control cells with antibodies to centromeric proteins (ACA) and HP1α. This experiment revealed that the HP1α rich regions which were stained brightly with DAPI frequently contain centromeric signals (Fig. 1C panels *a* and *b*). In contrast, DAPI and HP1α staining of the ChlR-depleted cells exhibited diffuse heterochromatin regions as compared to the control cells (Fig. 1C panels *c* and *d*). In addition, the centromere signals were scattered throughout the nucleus in ChlR-depleted cells (Fig. 1C panel *c*). Areas of overlapping HP1α and centromere signals, generating

yellow color, were clearly observed in the control cells but were smaller in ChlR-depleted cells (Fig. 1C panels *a* and *c*). To show the difference of heterochromatin foci quantitatively, we counted the number of heterochromatin foci per image with a diameter greater than 1.2 μm. While 76% of control cells had one or more heterochromatin foci of this size, only 39% of ChlR-depleted cells by #5 construct had similar foci (Fig. 1D). The average numbers of heterochromatin foci in these cells, as determined by this method were 2.4 and 0.7, respectively (Fig. S1). Cells depleted of ChlR using siRNA construct (#4) also showed a decreased heterochromatin number (0.9, Fig. S1). Thus, ChlR-depleted cells had fewer well-organized heterochromatin foci than control cells. This suggests that ChlR depletion might result in disorganized centromere localization in interphase cells.

To further examine chromatin distribution in the nucleus we performed live cell imaging studies using HeLa cells which stably express EGFP-histone H2B [23]. When unfixed control cells were examined on a confocal microscope, chromatin-dense regions were observed in both perinucleolar and perinuclear areas (Fig. 1E panel *a*, arrow and arrowhead). These EGFP-H2B chromatin rich regions were located in the same areas that were strongly stained with anti-HP1α antibody (Fig. 1C panel *a*). Contrary to this, in cells depleted of ChlR proteins the chromatin density was relatively homogenous throughout a nucleus, although there was some enrichment in the perinucleolar regions (Fig. 1E panels *b* and *c*). Thus, the several prominent heterochromatin regions are disrupted and lost within nuclei depleted of ChlR.

We also performed an immunofluorescence (IF) study on cells using the ACA antibody along with an antibody that recognizes histone H3 that is trimethylated at lysine 9 (H3K9-me3) since this post-translational histone modification is a marker of constitutive heterochromatin [16,33]. Maximum intensity projection (MIP) images were made from a series of Z stacks covering the entire nucleus to allow observation of all the centromere signals within a given cell. Most centromeres in control cells were contained in H3K9-me3-positive regions and were located in the perinuclear and perinucleolar regions (Fig. 1F panel *a*). Perinucleolar centromeres, presumably those of chromosomes carrying rDNA, were orderly arranged as a necklace-like string surrounding nucleoli (Fig. 1F inset). In ChlR-depleted cells centromeres were found throughout the nucleus, although these regions were still H3K9-me3-positive. However, the individual H3K9-me3-positive areas were smaller than those found in control cells (Fig. 1F panel *b*), which corresponded to the decreased size of heterochromatin foci detected by anti-HP1α antibody (Fig. 1C panel a). The majority of the centromeres were aberrantly localized in the areas between perinuclear and perinucleolar regions, where few centromeres were located in control cells. This was also obvious by standard fluorescence microscopy (Fig. 1C panel *c*). Furthermore, there were no typical necklace-like strings surrounding the nucleoli. To show the difference in the number of perinuclear centromeres quantitatively, we counted centromeres which were locating at the perinuclear region within 1.2 μm of the nuclear envelope. These data showed that while 29% centromeres in control cells were located in the perinuclear region, only 19% of the centromere in ChlR-depleted cells were within this region (Fig. 1G panel a). However, the total number of centromeres per image was higher in ChlR-depleted cells (17 in control and 22 in ChlR-depleted cells) (Fig. 1G panel b). Both of these differences between the control and ChlR-depleted cells were statistically significant ($p<0.0001$). Taken together, these data suggest that loss of ChlR in HeLa cells causes aberrant localization of heterochromatin and centromeres in the nucleus.

## Immunofluorescence analysis reveals decreased pericentric HP1α staining in the absence of ChlR although a substantial level of trimethyl-histone H3 at lysine 9 (H3K9-me3) is retained

To further confirm the aberration in HP1α localization at pericentric regions we performed experiments to observe the location of these HP1α dense regions on mitotic chromosomes. For these studies we treated cells with ZM447439 to inhibit the activity of aurora B kinase [36]. This treatment enabled us to visualize chromosome-associated HP1 by blocking the physiological removal of HP1 during mitosis by aurora B kinase [37,38]. To ensure that the treatment of HeLa cells with the aurora kinase inhibitor was completely effective, we used IF to detect the presence of histone H3 that was phosphorylated at serine 10 using an antibody that specifically detects this modification. Histone H3-serine 10 phosphorylation was completely abrogated by this treatment, indicating that aurora B kinase was completely inhibited (Fig. S2A panels *d* and *h*). While little HP1α was found at the centromeric regions of mitotic chromosomes in untreated control cells, treatment with ZM447439 followed by IF revealed discrete HP1α signals (Fig. S2A panels *e* and *g*, Fig. 2A panel *b*). In these ZM447439-treated cells, HP1α signals were clearly recognized on mitotic chromosomes, while most signals were excluded from the chromosomes and/or not recognized in the untreated cells. In the control ZM447439-treated cells the HP1α signals were adjacent to but did not completely overlap with the kinetochore signals demonstrating that HP1α was retained at pericentric heterochromatin regions (Fig. 2A panel *c* insets). Contrary to the control cells, mitotic ChlR-depleted cells did not show clear HP1α localization in either of ZM447439-treated or untreated cells (Fig. 2A panels *e* and *h* and data not shown). This was true for the cells transfected with two different shRNA expressing plasmids that target different regions of the mRNA. Quantitation of the intensity of pericentric HP1α signals was performed on the confocal images. For these analyses, 1.2 $\mu m^2$ regions of interest (ROIs) were set to encircle an entire single pericentric region (Fig. S2B). The average fluorescence intensities of HP1α signals in control cells and the cells depleted of ChlR1 by two siRNA constructs in the presence of ZM447439 were 70, 31 and 25, respectively (Fig. 2B). The difference between the value of control and ChlR1-depleted cells with the two different siRNA constructs was statistically significant by the Student's t-test ($p<0001$). When cells were not treated with the aurora kinase inhibitor, the fluorescence intensities were equally low in both the control and ChlR-depleted cells (Fig. 2B). Decreased retention of HP1γ, which also localizes weakly to centromeric heterochromatin in our experiments was also found in ChlR depleted cells (Fig. S3 panel f arrows). However, we did not observe a clear accumulation of pericentric HP1β signals even in the control cells treated with ZM447439 (Fig. S4 panel *f*). This could be because of the abundant presence of HP1β on chromosome arms as well as centromeric regions.

We then examined whether H3K9-me3 was present on mitotic chromosomes since this modification is required for HP1 recruitment to chromatin [17,18]. While the signal intensity of HP1α at pericentric regions was stronger in control cells than in ChlR-depleted cells, there was only a small difference in the signal intensity of H3K9-me3 between control and ChlR-depleted cells (Fig. 2C panels *c* and *f*). The data suggest that the chromatin association of HP1α and HP1γ, and possibly also HP1β, at pericentric regions is impaired when ChlR is depleted. However, a substantial level of the heterochromatin marker H3K9-me3 is retained without a dramatic reduction. Thus, localizations of the heterochromatin two markers HP1α and H3K9-me3 might be dissociated in the absence of ChlR at pericentric regions.

## Chromatin immunoprecipitation (ChIP) shows that HP1α and H3K9-me3 levels are decreased in pericentric region and at telomere in the absence of ChlR

In order to examine the impairment in the association of HP1 proteins with pericentric chromatin at a molecular level, we performed chromatin immunoprecipitations (ChIP). To

quantitate the amount of HP1α associated with pericentric repeat DNA, we used dot blot hybridization with $^{32}$P-labeled β-satellite sequence to compare the amount of immunoprecipitated DNA prepared from a control vector transfected HeLa clone (C1) and a ChlR-depleted HeLa clone (5.5). Clone 5.5 stably expressed a retroviral shRNA targeting ChlR which caused an almost complete depletion of the protein (Fig. 3A). The results showed a 48% relative recovery rate of β-satellite DNA associated with HP1α in ChlR-depleted cells as compared to control cells (Fig. 3C). For H3K9-me3, the relative recovery of β-satellite DNA was 87% upon ChlR depletion. Therefore, the absence of ChlR results in a marked decrease in the association of HP1α with β-satellite chromatin without significantly altering the binding of H3K9-me3, as predicted from the results of IF studies.

Telomeres are another major location of constitutive heterochromatin [39]. Therefore, we assessed HP1α-associated telomere sequences by applying $^{32}$P-labeled telomere sequence to the same blot. Since clone 5.5 has longer telomeres than the clone C1 (data not shown), the input signal from the ChlR1-depleted clone 5.5 was stronger than that from the control clone C1 (Fig. 3B). As opposed to the case of β-satellite, the recovery of both the HP1α and H3K9-me3 associated telomere sequence was reduced at 58 % and 41% in the clone 5.5 ChlR-depleted cells (Fig. 3C). Thus, the impairment of heterochromatin formation in telomeres is somehow different from that in pericentric regions. This difference might be attributable to an impairment of ChlR-dependent chromatin formation at the telomeres.

## Chromatin density at telomeres is decreased in the absence of ChlR

To address this possibility we performed a MNase assay to find out whether the aberrations in pericentric and telomeric chromatin in ChlR-depleted cells caused changes in DNA accessibility. DNA ladders resulting from the periodic digestion of chromatin at consecution of nucleosomes were visualized on an agarose gel after ethidium bromide (EtBr) staining followed by Southern blotting and hybridization with a β-satellite probe. Five days after the first transfection of shRNA-expression plasmids, control and ChlR-depleted cells exhibited identical EtBr staining (Fig. 4A left panel). There was also no substantial difference in the β-satellite hybridization between control and ChlR-depleted cells (Fig. 4A middle panel). This pattern was essentially the same as that obtained with the probes detecting satellite III, satellite 2, and *Alu* repeat DNA (Fig. S5). In contrast, the pattern was slightly different when a probe for telomere was used. The autoradiogram showed a diffuse smeary pattern in all the lanes, which was consistent with the previous data suggesting that telomeric DNA does not form a regular chromatin structure (Fig. 4A right panel) [40,41]. However, the content of longer polynucleosomes was diminished in ChlR-depleted cells. This was most obvious in the lanes containing chromatin from the 8-min or 12-min MNase digestions (Fig. 4A black arrows in right panel). The difference in the amount of polysomes in control and ChlR-depleted cells was also analyzed by densitometry using the phosphoimager (Fig. 4B). As expected, the chromatin densities obtained with β-satellite probe were not different between control and ChlR-depleted cells (Fig. 4B top panels). However, when telomere probe was used, the chromatin density of ChlR-depleted cells shifted to the right as compared to that of control (Fig. 4B bottom panels). This result suggests that the loss of ChlR might result in the alteration or impairment of telomeric chromatin formation.

## DNA methylation is decreased in Ddx11$^{-/-}$ mouse embryos

DNA methylation, specifically CpG dinucleotide methylation, is another hallmark of heterochromatin [42]. To examine whether there was any aberration in CpG methylation in ChlR-deficient cells, we extracted genomic DNA from mouse *Ddx11*$^{+/+}$ ES cells, E9.5 *Ddx11*$^{+/+}$ embryos and E9.5 *Ddx11*$^{-/-}$ embryos. The DNA was digested with the methylation-sensitive and resistant restriction endonucleases, *Hpa*II and *Msp*I, respectively, and the digests were analyzed by Southern hybridization with centromeric and pericentric

repeats probes. These probes recognize centromere repeats and pericentric repeats, generating 120-bp and 230-bp ladders, respectively. When the DNA was digested with *Msp*I, a methylation-resistant enzyme recognizing the DNA sequence CCGG regardless of its methylation status, all the digests showed similar hybridization patterns using probes for both minor and major satellite sequences indicating complete digestion (Fig. 5 lanes 4–6 and 10–12). In contrast, the genomic DNA treated with *Hpa*II, which cannot digest the methylated sequence, showed that while major satellite DNA from *Ddx11*$^{+/+}$ embryos was largely undigested, DNA from the *Ddx11*$^{-/-}$ embryos was digested well and ran as a 230-bp ladder which reached the bottom of the gel (Fig. 5, compare lanes 7 and 8 with lane 9). The fact that the band intensity of each step in the ladder in *Ddx11*$^{-/-}$ digests did not differ between *Hpa*II and *Msp*I digestions (Fig. 5 lanes 9 and 12) suggests that CpG methylation in this region of *Ddx11*$^{-/-}$ embryos is severely impaired. While the major satellite sequences comprise pericentric heterochromatin normally associated with HP1α, minor satellite sequences are a component of centromere repeats which are associated with kinetochore proteins such as CENP-A and CENP-B and are believed to have an euchromatic architecture [43]. This data suggests that only the heterochromatic regions of ChlR1 null chromosomes have impaired DNA methylation. Thus, ChlR-deficient regions of constitutive heterochromatin have aberrant properties in terms of epigenetic marks, namely HP1 localization and DNA methylation.

### ChlR and HP1 deficient cells exhibit similar phenotypes

Since loss of ChlR causes aberrant localization of HP1α and disorganized high-order heterochromatin, we postulated that loss of HP1 itself might also affect highly condensed regions of chromosomes in human cells. Therefore, we obtained a HeLa cell clone (H12) that expresses EGFP-histone H2B and is stably depleted of HP1α by infecting these cells with a retrovirus expressing shRNA targeting HP1α. Additionally, we transiently transfected these cells with a siRNA plasmid targeting HP1β to obtain combinations of HP1α– and/or HP1β-depleted cells. Immunoblot showed that both HP1 proteins were substantially depleted in these cells (Fig. 6A). We then examined chromatin density by visualizing EGFP localization in unfixed cells using a confocal microscope. Diffusely distributed chromatin was present in HP1β and HP1α/HP1β depleted cells while the control cells exhibited regions of bright EGFP fluorescence (Fig. 6B). Similar patterns were obtained when ChlR was depleted (Fig. 1E). Cells singly depleted of HP1α still showed brighter regions of EGFP fluorescence in perinuclear and perinucleolar regions. The localization of centromeres was also disorganized in cells depleted of both HP1α and HP1β (Fig. 6C) and resembled that of ChlR-depleted cells (Fig. 1F). Similar effects were obtained by additional shRNA targeting different region of HP1α (data not shown). This suggests that the HP1 isoforms associated with constitutive heterochromatin are required for the normal localization of centromere. These morphological data indicate that the ChlR depletion phenocopies HP1α/β depletion in terms of effects on high-order chromatin.

## Discussion

ChlR1 belongs to FANCJ helicase family, whose members have roles in genome integrity [2]. The studies in yeast CHL1 and mammalian ChlR1 indicate that CHL1/ChlR1 plays a role in sister-chromatid cohesion and contributes to chromosome-number stability [4–8]. The data of the present study support the conclusion that ChlR1 also affects epigenetic modifications and chromatin organization in the mammalian nucleus. Results from both morphological and molecular analyses demonstrate aberrations in the formation and localization of heterochromatin and in centromere localization in the absence of ChlR. This suggests that ChlR is required for normal heterochromatin organization. Furthermore, the data suggest that ChlR contributes to heterochromatin formation via effects on HP1

targeting and/or binding to the proper sites since both IF and ChIP data revealed a dramatic decrease in pericentric HP1α in ChlR-depleted cells. This hypothesis is further supported by our data showing that depletion of HP1 proteins, especially both HP1α and HP1β, caused similar global morphological aberrations. Therefore, we conclude that ChlR has a role in targeting of HP1 to the correct genomic regions and that proper localization and binding of HP1 proteins is required for the global organization of heterochromatin and centromere clustering.

HP1 was initially identified in *Drosophila melanogaster* as a protein that predominantly localized to the chromocenter of polytene chromosomes [44,45]. Mammals have 3 HP1 isoforms, HP1α, HP1β, and HP1γ [20]. HP1α is exclusively localized in constitutive heterochromatin and HP1β is less strictly found in heterochromatin, while HP1γ localizes in euchromatic sites [46,47]. All have 3 common domains, chromodomain (CD), a hinge region, and chromoshadow domain (CSD) [20]. In constitutive heterochromatin, the N-terminus portion of histone H3 is methylated at lysine 9 by specific histone methyltransferases, SUV39H1 and SUV39H2 [48]. HP1 preferentially binds to methylated H3 at lysine 9 (HeK9-me) through its CD [17,18]. Our IF data show that the level of pericentric H3K9-me3 was not markedly decreased in the absence of ChlR. While our ChIP data revealed that the level of both H3K9-me3 and HP1α are decreased at β-satellite and telomeric heterochromatin in response to ChlR depletion, the decrease in HP1α was greater. These data collectively suggest that ChlR could be involved in heterochromatin formation and its absence might cause heterochromatin malformation at the steps of H3K9-me3 and HP1α localization.

To date the major function that has been attributed to CHL1 is a role in sister chromatid cohesion. Studies in budding yeast suggest that CHL1 might be involved in the process of cohesion establishment, a process that is coupled with DNA replication [6,49]. Indeed, CHL1 was found to be associated with CTF7 [6], a cohesion establishment factor carrying acetyltransferase activity [50–52]. In both budding yeast and fission yeast, *chl1* and *ctf18* are synthetic lethal [5,53]. CTF18 is a component of the replication factor C (RFC) complex which is specific for the establishment of [54]. CHL1 is also physically associated with PCNA, an essential molecule for DNA replication [55]. Therefore, CHL1 is associated with the proteins involved in DNA replication which specifically function in cohesion establishment. These published data support the conclusion that CHL1 is involved in the establishment of sister-chromatid cohesion during DNA replication. Although biochemical data on mammalian ChlR are sparse, our data also indicated that human ChlR could bind to a fragment of human CTF7 and DCC1, another component of the CTF18-RFC complex (unpublished data). Additionally, ChlR associates with flap endonuclease-1 (FEN1), which is a factor required for lagging strand maturation [56]. This suggests that ChlR might collaborate with FEN1 in trimming lagging strands in replication forks, which would enable a replication fork to pass through the pre-loaded cohesin ring smoothly [57]. This in turn may contribute to the complete establishment of cohesion. The study also showed that ChlR binds to PCNA in human cells. PCNA could serve as a platform for both ChlR and FEN1 as well as many other replication-related molecules [58]. These results strongly suggest that mammalian ChlR might function in cohesion establishment by collaborating with the proteins involved in DNA replication especially lagging strand replication. In support of this hypothesis, a comprehensive genetic study in yeast found that *CHL1* made an epistasis group with *TOF1*, *CSM3* and *CTF4* [59]. CTF4 is a molecule bridging the MCM helicase and DNA polymerase α, a lagging-strand specific polymerase, which is consistent with a hypothetical role for CHL1/ChlR in lagging strand replication and cohesion establishment in collaboration with FEN1 [57]. The question is how ChlR can contribute to the proper loading or targeting of HP1 to the correct chromosomal sites. Our efforts in demonstrating a physical association between ChlR and HP1 have been unsuccessful (unpublished data).

This suggests that ChlR may function indirectly. Obviously, further studies are required to elucidate the exact mechanism of ChlR function in heterochromatin formation.

Is there any linkage between the role of ChlR in cohesion establishment during DNA replication and heterochromatin formation? Proteins and protein complexes associated with chromatin are an obstacle for the replisome. One of these complexes most likely is the preloaded cohesin complex. The cohesin complex makes a ring structure composed of SMC1, SMC3, SCC1, and either SA1 or SA2 [60]. When the replisome is passing through the cohesin ring, the replication machinery cannot move smoothly because the size of the replisome is much larger than that of the diameter of a cohesin ring (>100 nm vs. 30–40 nm) [61]. Farina and others have hypothesized that FEN1 and ChlR support this process [57]. HP1 proteins in constitutive heterochromatin are another obstacle [62]. The attachment of HP1 to chromatin is normally mediated by H3K9-me-CD interaction. However, upon the DNA/chromatin replication the association of HP1 with chromatin at the replication sites is no longer dependent of the H3K9-me3-CD interaction but requires another protein complex, CAF-1 [63]. The largest subunit of CAF-1, p150, binds to PCNA at the replication fork and simultaneously binds to HP1 [64]. CAF-1's primary role is to incorporate core histones into newly replicated DNA to produce the complete chromatin. When p150 subunit is depleted in mouse embryo fibroblasts (MEFs), cell cycle progression is delayed at late S-phase, the time when constitutive heterochromatin is replicated [62]. This delay is rescued by expression of wild-type p150 but not by a mutant p150 lacking the binding ability to HP1 [62]. Importantly, *Suv39h1*$^{-/-}$*Suv39h2*$^{-/-}$ MEFs do not delay in late S-phase upon p150 depletion. Since HP1 is not bound to the proper site in these cells, this suggests that heterochromatin is less of a replication obstacle when HP1 is not bound to the proper sites. These data strongly imply that the presence of HP1 at the constitutive heterochromatin is an obstacle for the DNA replication. One possibility suggested by the published data and our current data is that ChlR might function in facilitating DNA replication at difficult sites such as cohesion binding sites and constitutive heterochromatin and that ChlR might participate in both cohesion establishment and heterochromatin formation. ChlR might unwind DNA strands at cohesion sites and in heterochromatin or enhance the ability of FEN1 to DNA strands at these sites as proposed by Farina et al. [57].

At the time of constitutive heterochromatin replication HP1 binds to the DNMT1 and DNMT3a DNA methyltransferases [42] which methylate the cytosine nucleotides in the context of CpG as these sequences are replicated. Our data on centromeric DNA methylation in *Ddx11*$^{-/-}$ embryos support the theory that ChlR plays a role in methylation of centromeric/heterochromatin regions. Whereas the major satellite repeats in pericentric heterochromatin are characterized by the presence of H3K9-me and HP1, the minor satellite repeats which compose the centromere/kinetochore regions are characterized by their association with kinetochore proteins such as CENP-A and CENP-B. They also do not have H3K9-m3 and are believed to be rather euchromatic [43]. The DNA methylation data obtained in this study showed a dramatic difference between major and minor satellites. Methylation was severely impaired in the major repeats but not in minor repeats. This data further support the hypothesis that ChlR plays a heterochromatin-specific role in epigenetic genomic events.

The current data present the possibility that ChlR might contribute to sister-chromatid cohesion through recruiting HP1 to heterochromatin. The role of *Swi6*, the *Schizosaccharomyces pombe* ortholog of mammalian HP1, in heterochromatin formation and sister-chromatid cohesion is well established [65]. Swi6 is located in the outer repeats of centromeres [66,67], which are considered to be equivalent to the pericentric heterochromatin in mammals. This localization is mediated by H3K9-me which is catalyzed by Clr4, the histone H3 acetyltransferase in fission yeast [18,68]. Both Swi6 and Clr4 are

required for enrichment of cohesin in outer repeats [69,70]. Since Swi6 and Psc3 (the ortholog of SCC3) interact directly, it is believed that Swi6 recruits cohesins to the outer repeats of centromeres, where centromeric cohesion is made [70]. Furthermore, it is established that Swi6 also contributes to centromeric localization of Sgo1, which is known to have a role in protecting cohesin from the cohesin-removing activity of PLK1 mitotic kinase [71,72]. Thus, in fission yeast Swi6 has dual roles in contributing cohesion, recruiting cohesins and protection of cohesin through Sgo1 localization. In mammals, various proteins have the consensus motif, PXVXL/I, which mediates association with HP1's CSD. Among them, NIPBL, a cohesin-loading factor, is of particular importance in terms of sister-chromatid cohesion. Depletion of this in HeLa cells leads to precocious separation of sister chromatids in mitosis [73]. The *in vitro* association of a fragment of NIPBL and HP1 has also been documented [22]. Therefore, it is reasonable to postulate that HP1 might have a role in cohesion by recruiting cohesion-related molecules to the proper sites. In mouse cells, pericentric regions are the sites of centromeric cohesion [74]. MEFs lacking both genes of *Suv39h* (*Suv39h1*$^{-/-}$: *Suv39h2*$^{-/-}$), the histone methyltransferase generating H3K9-me, have chromatid pairs carrying separated centromeres, an indicator of cohesion defects [74]. Additionally, defects in centromeric cohesion were shown in wild-type MEFs treated with a HDAC inhibitor, which abrogated H3K9-me [75]. It has also been shown that siRNA depletion of HP1α [76], and over-expression of a dominant-negative mutant of HP1 in HeLa cells causes centromeric cohesion effect [77]. However, other studies by Serrano et al. reported that there was no mitotic aberrations even in the absence of HP1α and HP1β [78]. There are also contradictory reports on cohesin retention at mitotic centromeres. Koch et al. and Serrano et al. reported that there was no reduction of cohesin enrichment in mitotic centromeres in the absence of *Suv39h* or HP1, respectively [75,78]. Based on the assumption that HP1 might be required for the protection of centromeric cohesion as in fission yeast, Yamagishi et al. showed a marked impairment of centromeric cohesion in HeLa cells lacking HP1α [76]. However, a recent study revealed that although Sgo1 can bind to HP1 through the interaction of its PXVXL/I motif with the HP1's CSD, HP1 was not necessary for either the centromeric localization of Sgo1 or centromeric cohesion [79]. Because of these serious controversies, it is not clear whether HP1 is directly required for sister-chromatid cohesion at centromeres and further studies are needed to resolve this issue.

Inherited diseases caused by mutations in cohesins and cohesion-related genes are collectively called cohesinopathies [10]. The two most common cohesinopathies are, Cornelia de Lange syndrome (CdLS), which is caused by mutations of *SMC1*, *SMC3*, or *NIPBL* [80–83] and Roberts/SC phocomedia syndrome which is caused by *ESCO2* mutations, a human ortholog of *CTF7* [84]. Recently, a new cohesinopathy, WABS, was found to be due to *DDX11*-deficiency [9]. All three of these cohesinopathies are characterized by a variety of developmental defects, including growth and mental retardation, limb deformities, and craniofacial anomalies [10]. The wide range of phenotypic abnormalities displayed by these patients is thought to be due to effects of cohesins and cohesin-related genes on gene expression/accessibility during embryogenesis. Therefore, we postulate that ChlR1 may also play a role in gene expression during embryogenesis. The observation that yeast *chl1* mutants show both an increase and decrease in gene silencing in different genomic locations, which seemed to be dependent on the status of Sir2 silencing protein further supports this hypothesis [13]. In this sense, it is of interest to examine gene-expression patterns in *Ddx11*$^{-/-}$ embryos to identify the genes aberrantly expressed after implantation. Since *Ddx11* null embryos die from placental defect around E10.5 it will also be interesting to examine gene-expression patterns in *Ddx11*$^{-/-}$ placenta since this may allow us to understand the role of ChlR in the normal placental development.

It is well established that ChlR1 is required for sister-chromatid cohesion and thereby functions in the maintenance of genomic integrity. Additionally, ChlR1 is involved in the

stable maintenance of papillomavirus genome copy number in mammalian cells [85]. In this study we further show that ChlR1 has a role in high-order nuclear organization. Thus, ChlR1, like yeast CHL1, has pleiotropic roles in mammalian nuclear functions.

## Supplementary Material

Refer to Web version on PubMed Central for supplementary material.

## Acknowledgments

The authors are grateful to Dr. Stephen Smale, University of California Los Angeles, for providing anti-HP1α antibody; Dr. Kevin Sullivan, National University of Ireland Galway, for the EGFP-H2B-expessing HeLa cell line; Dr. Stanley Cohen, Stanford University, for the probes of human repetitive sequences; Dr. Nicholas Keen, AstraZeneca, for ZM447439 and Dr. Brian Freiberg, Samuel Connell, and Dr. Jennifer Peters, St. Jude Children's Research Hospital, for helpful technical advice. We also thank Dr. Sarah Elgin, Washington University in St. Louis, for helpful comments. The authors are grateful to the members of Lahti's laboratory for their assistance and useful suggestions. This work was funded by support from ALSAC (American Syrian Lebanese Associated Charities) and Comprehensive Cancer Center Support Grant CA021765 from the National Institute of Health.

## Reference List

1. Amann J, Kidd VJ, Lahti JM. Characterization of putative human homologues of the yeast chromosome transmission fidelity gene, CHL1. J Biol Chem. 1997; 272:3823–3832. [PubMed: 9013641]
2. Wu Y, Suhasini AN, Brosh RM Jr. Welcome the family of FANCJ-like helicases to the block of genome stability maintenance proteins. Cell Mol Life Sci. 2009; 66:1209–1222. [PubMed: 19099189]
3. Amann J, Valentine M, Kidd VJ, Lahti JM. Localization of chi1-related helicase genes to human chromosome regions 12p11 and 12p13: similarity between parts of these genes and conserved human telomeric-associated DNA. Genomics. 1996; 32:260–265. [PubMed: 8833153]
4. Gerring SL, Spencer F, Hieter P. The CHL 1 (CTF 1) gene product of Saccharomyces cerevisiae is important for chromosome transmission and normal cell cycle progression in G2/M. EMBO J. 1990; 9:4347–4358. [PubMed: 2265610]
5. Mayer ML, Pot I, Chang M, Xu H, Aneliunas V, Kwok T, Newitt R, Aebersold R, Boone C, Brown GW, Hieter P. Identification of protein complexes required for efficient sister chromatid cohesion. Mol Biol Cell. 2004; 15:1736–1745. [PubMed: 14742714]
6. Skibbens RV. Chl1p, a DNA helicase-like protein in budding yeast, functions in sister-chromatid cohesion. Genetics. 2004; 166:33–42. [PubMed: 15020404]
7. Parish JL, Rosa J, Wang X, Lahti JM, Doxsey SJ, Androphy EJ. The DNA helicase ChlR1 is required for sister chromatid cohesion in mammalian cells. J Cell Sci. 2006; 119:4857–4865. [PubMed: 17105772]
8. Inoue A, Li T, Roby SK, Valentine MB, Inoue M, Boyd K, Kidd VJ, Lahti JM. Loss of ChlR1 helicase in mouse causes lethality due to the accumulation of aneuploid cells generated by cohesion defects and placental malformation. Cell Cycle. 2007; 6:1646–1654. [PubMed: 17611414]
9. van der Lelij P, Chrzanowska KH, Godthelp BC, Rooimans MA, Oostra AB, Stumm M, Zdzienicka MZ, Joenje H, De Winter JP. Warsaw breakage syndrome, a cohesinopathy associated with mutations in the XPD helicase family member DDX11/ChlR1. Am J Hum Genet. 2010; 86:262–266. [PubMed: 20137776]
10. Liu J, Krantz ID. Cohesin and human disease. Annu Rev Genomics Hum Genet. 2008; 9:303–320. [PubMed: 18767966]
11. Bose T, Gerton JL. Cohesinopathies, gene expression, and chromatin organization. J Cell Biol. 2010; 189:201–210. [PubMed: 20404106]
12. Phillips JE, Corces VG. CTCF: master weaver of the genome. Cell. 2009; 137:1194–1211. [PubMed: 19563753]

13. Das SP, Sinha P. The budding yeast protein Chl1p has a role in transcriptional silencing, rDNA recombination, and aging. Biochem Biophys Res Commun. 2005; 337:167–172. [PubMed: 16182251]
14. Blander G, Guarente L. The Sir2 family of protein deacetylases. Annu Rev Biochem. 2004; 73:417–435. [PubMed: 15189148]
15. Huisinga KL, Brower-Toland B, Elgin SC. The contradictory definitions of heterochromatin: transcription and silencing. Chromosoma. 2006; 115:110–122. [PubMed: 16506022]
16. Peters AH, O'Carroll D, Scherthan H, Mechtler K, Sauer S, Schofer C, Weipoltshammer K, Pagani M, Lachner M, Kohlmaier A, Opravil S, Doyle M, Sibilia M, Jenuwein T. Loss of the Suv39h histone methyltransferases impairs mammalian heterochromatin and genome stability. Cell. 2001; 107:323–337. [PubMed: 11701123]
17. Lachner M, O'Carroll D, Rea S, Mechtler K, Jenuwein T. Methylation of histone H3 lysine 9 creates a binding site for HP1 proteins. Nature. 2001; 410:116–120. [PubMed: 11242053]
18. Bannister AJ, Zegerman P, Partridge JF, Miska EA, Thomas JO, Allshire RC, Kouzarides T. Selective recognition of methylated lysine 9 on histone H3 by the HP1 chromo domain. Nature. 2001; 410:120–124. [PubMed: 11242054]
19. Lomberk G, Wallrath L, Urrutia R. The Heterochromatin Protein 1 family. Genome Biol. 2006; 7:228. [PubMed: 17224041]
20. Maison C, Almouzni G. HP1 and the dynamics of heterochromatin maintenance. Nat Rev Mol Cell Biol. 2004; 5:296–304. [PubMed: 15071554]
21. Maison C, Bailly D, Peters AH, Quivy JP, Roche D, Taddei A, Lachner M, Jenuwein T, Almouzni G. Higher-order structure in pericentric heterochromatin involves a distinct pattern of histone modification and an RNA component. Nat Genet. 2002; 30:329–334. [PubMed: 11850619]
22. Lechner MS, Schultz DC, Negorev D, Maul GG, Rauscher FJ III. The mammalian heterochromatin protein 1 binds diverse nuclear proteins through a common motif that targets the chromoshadow domain. Biochem Biophys Res Commun. 2005; 331:929–937. [PubMed: 15882967]
23. Kanda T, Sullivan KF, Wahl GM. Histone-GFP fusion protein enables sensitive analysis of chromosome dynamics in living mammalian cells. Curr Biol. 1998; 8:377–385. [PubMed: 9545195]
24. Todorov IT, Attaran A, Kearsey SE. BM28, a human member of the MCM2-3-5 family, is displaced from chromatin during DNA replication. J Cell Biol. 1995; 129:1433–1445. [PubMed: 7790346]
25. Fey EG, Krochmalnic G, Penman S. The nonchromatin substructures of the nucleus: the ribonucleoprotein (RNP)-containing and RNP-depleted matrices analyzed by sequential fractionation and resinless section electron microscopy. J Cell Biol. 1986; 102:1654–1665. [PubMed: 3700470]
26. Goodarzi AA, Noon AT, Deckbar D, Ziv Y, Shiloh Y, Lobrich M, Jeggo PA. ATM signaling facilitates repair of DNA double-strand breaks associated with heterochromatin. Mol Cell. 2008; 31:167–177. [PubMed: 18657500]
27. Demuth I, Digweed M, Concannon P. Human SNM1B is required for normal cellular response to both DNA interstrand crosslink-inducing agents and ionizing radiation. Oncogene. 2004; 23:8611–8618. [PubMed: 15467758]
28. Freibaum BD, Counter CM. The protein hSnm1B is stabilized when bound to the telomere-binding protein TRF2. J Biol Chem. 2008; 283:23671–23676. [PubMed: 18593705]
29. Freibaum BD, Counter CM. The protein hSnm1B is stabilized when bound to the telomere-binding protein TRF2. J Biol Chem. 2008; 283:23671–23676. [PubMed: 18593705]
30. Ten Hagen KG, Cohen SN. Timing of replication of beta satellite repeats of human chromosomes. Nucleic Acids Res. 1993; 21:2139–2142. [PubMed: 8502554]
31. de Lange T. Human telomeres are attached to the nuclear matrix. EMBO J. 1992; 11:717–724. [PubMed: 1537344]
32. Narita M, Nunez S, Heard E, Narita M, Lin AW, Hearn SA, Spector DL, Hannon GJ, Lowe SW. Rb-mediated heterochromatin formation and silencing of E2F target genes during cellular senescence. Cell. 2003; 113:703–716. [PubMed: 12809602]

33. Wu R, Terry AV, Singh PB, Gilbert DM. Differential subnuclear localization and replication timing of histone H3 lysine 9 methylation states. Mol Biol Cell. 2005; 16:2872–2881. [PubMed: 15788566]
34. Sonoda E, Matsusaka T, Morrison C, Vagnarelli P, Hoshi O, Ushiki T, Nojima K, Fukagawa T, Waizenegger IC, Peters JM, Earnshaw WC, Takeda S. Scc1/Rad21/Mcd1 is required for sister chromatid cohesion and kinetochore function in vertebrate cells. Dev Cell. 2001; 1:759–770. [PubMed: 11740938]
35. Taddei A, Roche D, Sibarita JB, Turner BM, Almouzni G. Duplication and maintenance of heterochromatin domains. J Cell Biol. 1999; 147:1153–1166. [PubMed: 10601331]
36. Ditchfield C, Johnson VL, Tighe A, Ellston R, Haworth C, Johnson T, Mortlock A, Keen N, Taylor SS. Aurora B couples chromosome alignment with anaphase by targeting BubR1, Mad2, and Cenp-E to kinetochores. J Cell Biol. 2003; 161:267–280. [PubMed: 12719470]
37. Fischle W, Tseng BS, Dormann HL, Ueberheide BM, Garcia BA, Shabanowitz J, Hunt DF, Funabiki H, Allis CD. Regulation of HP1-chromatin binding by histone H3 methylation and phosphorylation 2. Nature. 2005; 438:1116–1122. [PubMed: 16222246]
38. Hirota T, Lipp JJ, Toh BH, Peters JM. Histone H3 serine 10 phosphorylation by Aurora B causes HP1 dissociation from heterochromatin 3. Nature. 2005; 438:1176–1180. [PubMed: 16222244]
39. Blasco MA. The epigenetic regulation of mammalian telomeres. Nat Rev Genet. 2007; 8:299–309. [PubMed: 17363977]
40. Makarov VL, Lejnine S, Bedoyan J, Langmore JP. Nucleosomal organization of telomere-specific chromatin in rat. Cell. 1993; 73:775–787. [PubMed: 8500170]
41. Tommerup H, Dousmanis A, de Lange T. Unusual chromatin in human telomeres. Mol Cell Biol. 1994; 14:5777–5785. [PubMed: 8065312]
42. Cedar H, Bergman Y. Linking DNA methylation and histone modification: patterns and paradigms. Nat Rev Genet. 2009; 10:295–304. [PubMed: 19308066]
43. Blower MD, Sullivan BA, Karpen GH. Conserved organization of centromeric chromatin in flies and humans. Dev Cell. 2002; 2:319–330. [PubMed: 11879637]
44. James TC, Elgin SC. Identification of a nonhistone chromosomal protein associated with heterochromatin in Drosophila melanogaster and its gene. Mol Cell Biol. 1986; 6:3862–3872. [PubMed: 3099166]
45. James TC, Eissenberg JC, Craig C, Dietrich V, Hobson A, Elgin SC. Distribution patterns of HP1, a heterochromatin-associated nonhistone chromosomal protein of Drosophila. Eur J Cell Biol. 1989; 50:170–180. [PubMed: 2515059]
46. Minc E, Courvalin JC, Buendia B. HP1gamma associates with euchromatin and heterochromatin in mammalian nuclei and chromosomes. Cytogenet Cell Genet. 2000; 90:279–284. [PubMed: 11124534]
47. Nielsen AL, Oulad-Abdelghani M, Ortiz JA, Remboutsika E, Chambon P, Losson R. Heterochromatin formation in mammalian cells: interaction between histones and HP1 proteins. Mol Cell. 2001; 7:729–739. [PubMed: 11336697]
48. Rea S, Eisenhaber F, O'Carroll D, Strahl BD, Sun ZW, Schmid M, Opravil S, Mechtler K, Ponting CP, Allis CD, Jenuwein T. Regulation of chromatin structure by site-specific histone H3 methyltransferases. Nature. 2000; 406:593–599. [PubMed: 10949293]
49. Petronczki M, Chwalla B, Siomos MF, Yokobayashi S, Helmhart W, Deutschbauer AM, Davis RW, Watanabe Y, Nasmyth K. Sister-chromatid cohesion mediated by the alternative RF-CCtf18/Dcc1/Ctf8, the helicase Chl1 and the polymerase-alpha-associated protein Ctf4 is essential for chromatid disjunction during meiosis II. J Cell Sci. 2004; 117:3547–3559. [PubMed: 15226378]
50. Skibbens RV, Corson LB, Koshland D, Hieter P. Ctf7p is essential for sister chromatid cohesion and links mitotic chromosome structure to the DNA replication machinery. Genes Dev. 1999; 13:307–319. [PubMed: 9990855]
51. Toth A, Ciosk R, Uhlmann F, Galova M, Schleiffer A, Nasmyth K. Yeast cohesin complex requires a conserved protein, Eco1p(Ctf7), to establish cohesion between sister chromatids during DNA replication. Genes Dev. 1999; 13:320–333. [PubMed: 9990856]

52. Ben-Shahar TR, Heeger S, Lehane C, East P, Flynn H, Skehel M, Uhlmann F. Eco1-dependent cohesin acetylation during establishment of sister chromatid cohesion. Science. 2008; 321:563–566. [PubMed: 18653893]
53. Ansbach AB, Noguchi C, Klansek IW, Heidlebaugh M, Nakamura TM, Noguchi E. RFCCtf18 and the Swi1-Swi3 complex function in separate and redundant pathways required for the stabilization of replication forks to facilitate sister chromatid cohesion in Schizosaccharomyces pombe. Mol Biol Cell. 2008; 19:595–607. [PubMed: 18045993]
54. Mayer ML, Gygi SP, Aebersold R, Hieter P. Identification of RFC(Ctf18p, Ctf8p, Dcc1p): an alternative RFC complex required for sister chromatid cohesion in S. cerevisiae. Mol Cell. 2001; 7:959–970. [PubMed: 11389843]
55. Moldovan GL, Pfander B, Jentsch S. PCNA controls establishment of sister chromatid cohesion during S phase. Mol Cell. 2006; 23:723–732. [PubMed: 16934511]
56. Kao HI, Campbell JL, Bambara RA. Dna2p helicase/nuclease is a tracking protein, like FEN1, for flap cleavage during Okazaki fragment maturation. J Biol Chem. 2004; 279:50840–50849. [PubMed: 15448135]
57. Farina A, Shin JH, Kim DH, Bermudez VP, Kelman Z, Seo YS, Hurwitz J. Studies with the human cohesin establishment factor, ChlR1. Association of ChlR1 with Ctf18-RFC and Fen1. J Biol Chem. 2008; 283:20925–20936. [PubMed: 18499658]
58. Moldovan GL, Pfander B, Jentsch S. PCNA, the maestro of the replication fork. Cell. 2007; 129:665–679. [PubMed: 17512402]
59. Xu H, Boone C, Brown GW. Genetic dissection of parallel sister-chromatid cohesion pathways. Genetics. 2007; 176:1417–1429. [PubMed: 17483413]
60. Hirano T. Chromosome cohesion, condensation, and separation. Annu Rev Biochem. 2000; 69:115–144. [PubMed: 10966455]
61. Bylund GO, Burgers PM. Replication protein A-directed unloading of PCNA by the Ctf18 cohesion establishment complex. Mol Cell Biol. 2005; 25:5445–5455. [PubMed: 15964801]
62. Quivy JP, Gerard A, Cook AJ, Roche D, Almouzni G. The HP1-p150/CAF-1 interaction is required for pericentric heterochromatin replication and S-phase progression in mouse cells. Nat Struct Mol Biol. 2008; 15:972–979. [PubMed: 19172751]
63. Quivy JP, Roche D, Kirschner D, Tagami H, Nakatani Y, Almouzni G. A CAF-1 dependent pool of HP1 during heterochromatin duplication. EMBO J. 2004; 23:3516–3526. [PubMed: 15306854]
64. Murzina N, Verreault A, Laue E, Stillman B. Heterochromatin dynamics in mouse cells: interaction between chromatin assembly factor 1 and HP1 proteins. Mol Cell. 1999; 4:529–540. [PubMed: 10549285]
65. Peters JM, Tedeschi A, Schmitz J. The cohesin complex and its roles in chromosome biology. Genes Dev. 2008; 22:3089–3114. [PubMed: 19056890]
66. Nakayama J, Klar AJ, Grewal SI. A chromodomain protein, Swi6, performs imprinting functions in fission yeast during mitosis and meiosis. Cell. 2000; 101:307–317. [PubMed: 10847685]
67. Partridge JF, Borgstrom B, Allshire RC. Distinct protein interaction domains and protein spreading in a complex centromere. Genes Dev. 2000; 14:783–791. [PubMed: 10766735]
68. Nakayama J, Rice JC, Strahl BD, Allis CD, Grewal SI. Role of histone H3 lysine 9 methylation in epigenetic control of heterochromatin assembly. Science. 2001; 292:110–113. [PubMed: 11283354]
69. Bernard P, Maure JF, Partridge JF, Genier S, Javerzat JP, Allshire RC. Requirement of heterochromatin for cohesion at centromeres. Science. 2001; 294:2539–2542. [PubMed: 11598266]
70. Nonaka N, Kitajima T, Yokobayashi S, Xiao G, Yamamoto M, Grewal SI, Watanabe Y. Recruitment of cohesin to heterochromatic regions by Swi6/HP1 in fission yeast. Nat Cell Biol. 2002; 4:89–93. [PubMed: 11780129]
71. Kitajima TS, Kawashima SA, Watanabe Y. The conserved kinetochore protein shugoshin protects centromeric cohesion during meiosis. Nature. 2004; 427:510–517. [PubMed: 14730319]
72. Kitajima TS, Sakuno T, Ishiguro K, Iemura S, Natsume T, Kawashima SA, Watanabe Y. Shugoshin collaborates with protein phosphatase 2A to protect cohesin. Nature. 2006; 441:46–52. [PubMed: 16541025]

73. Watrin E, Schleiffer A, Tanaka K, Eisenhaber F, Nasmyth K, Peters JM. Human Scc4 is required for cohesin binding to chromatin, sister-chromatid cohesion, and mitotic progression. Curr Biol. 2006; 16:863–874. [PubMed: 16682347]
74. Guenatri M, Bailly D, Maison C, Almouzni G. Mouse centric and pericentric satellite repeats form distinct functional heterochromatin. J Cell Biol. 2004; 166:493–505. [PubMed: 15302854]
75. Koch B, Kueng S, Ruckenbauer C, Wendt KS, Peters JM. The Suv39h-HP1 histone methylation pathway is dispensable for enrichment and protection of cohesin at centromeres in mammalian cells. Chromosoma. 2008; 117:199–210. [PubMed: 18075750]
76. Yamagishi Y, Sakuno T, Shimura M, Watanabe Y. Heterochromatin links to centromeric protection by recruiting shugoshin. Nature. 2008; 455:251–255. [PubMed: 18716626]
77. Inoue A, Hyle J, Lechner MS, Lahti JM. Perturbation of HP1 localization and chromatin binding ability causes defects in sister-chromatid cohesion. Mutat Res. 2008; 657:48–55. [PubMed: 18790078]
78. Serrano A, Rodriguez-Corsino M, Losada A. Heterochromatin protein 1 (HP1) proteins do not drive pericentromeric cohesin enrichment in human cells. PLoS One. 2009; 4:e5118. [PubMed: 19352502]
79. Kang J, Chaudhary J, Dong H, Kim S, Brautigam CA, Yu H. Mitotic Centromeric Targeting of HP1 and Its Binding to Sgo1 Are Dispensable for Sister-Chromatid Cohesion in Human Cells. Mol Biol Cell. 2011
80. Krantz ID, McCallum J, DeScipio C, Kaur M, Gillis LA, Yaeger D, Jukofsky L, Wasserman N, Bottani A, Morris CA, Nowaczyk MJ, Toriello H, Bamshad MJ, Carey JC, Rappaport E, Kawauchi S, Lander AD, Calof AL, Li HH, Devoto M, Jackson LG. Cornelia de Lange syndrome is caused by mutations in NIPBL, the human homolog of Drosophila melanogaster Nipped-B. Nat Genet. 2004; 36:631–635. [PubMed: 15146186]
81. Tonkin ET, Wang TJ, Lisgo S, Bamshad MJ, Strachan T. NIPBL, encoding a homolog of fungal Scc2-type sister chromatid cohesion proteins and fly Nipped-B, is mutated in Cornelia de Lange syndrome. Nat Genet. 2004; 36:636–641. [PubMed: 15146185]
82. Musio A, Selicorni A, Focarelli ML, Gervasini C, Milani D, Russo S, Vezzoni P, Larizza L. X-linked Cornelia de Lange syndrome owing to SMC1L1 mutations. Nat Genet. 2006; 38:528–530. [PubMed: 16604071]
83. Deardorff MA, Kaur M, Yaeger D, Rampuria A, Korolev S, Pie J, Gil-Rodriguez C, Arnedo M, Loeys B, Kline AD, Wilson M, Lillquist K, Siu V, Ramos FJ, Musio A, Jackson LS, Dorsett D, Krantz ID. Mutations in cohesin complex members SMC3 and SMC1A cause a mild variant of cornelia de Lange syndrome with predominant mental retardation. Am J Hum Genet. 2007; 80:485–494. [PubMed: 17273969]
84. Vega H, Waisfisz Q, Gordillo M, Sakai N, Yanagihara I, Yamada M, van GD, Kayserili H, Xu C, Ozono K, Jabs EW, Inui K, Joenje H. Roberts syndrome is caused by mutations in ESCO2, a human homolog of yeast ECO1 that is essential for the establishment of sister chromatid cohesion. Nat Genet. 2005; 37:468–470. [PubMed: 15821733]
85. Parish JL, Bean AM, Park RB, Androphy EJ. ChlR1 is required for loading papillomavirus E2 onto mitotic chromosomes and viral genome maintenance. Mol Cell. 2006; 24:867–876. [PubMed: 17189189]

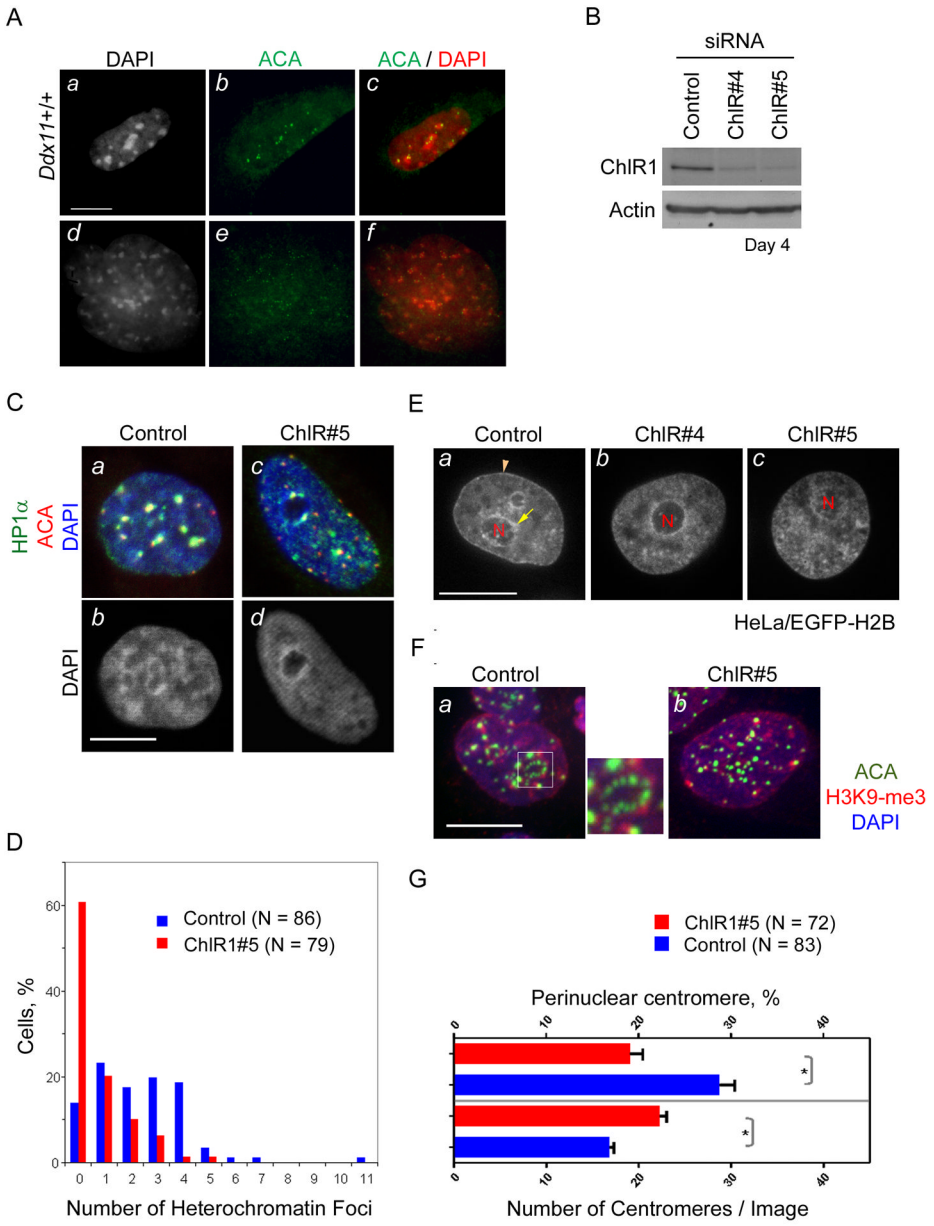


**Figure 1.**

ChlR-deficient mouse and human cells exhibit disorganized heterochromatin and aberrant high-order nuclear structure. (A) *Ddx11*$^{-/-}$ cells show dispersed heterochromatin and abnormal centromere localization. The DAPI signal is artificially converted into red in *c* and *f*. (B) Immunoblot showing protein depletion of ChlR in HeLa cells 4 days after the transfection of two siRNA expression plasmids targeting ChlR. (C) ChlR-depleted HeLa cells have obscure perinuclear and perinucleolar heterochromatin as revealed by anti-HP1α and DAPI staining. (D) ChlR1-depleted cells have fewer heterochromatin foci. Heterochromatin foci showing a HP1α signal with diameter greater than 1.2 μm were enumerated. (E) ChlR-depleted EGFP-H2B expressing HeLa cells have diffuse chromatin-dense regions which are distributed throughout a nucleus. The arrow and arrowhead indicate perinucleolar and perinuclear regions, respectively. N depicts a nucleolus. (F) Localization of centromeres and trimethyl-histone H3 at lysine 9 (H3K9-me3) in EGFP-H2B-expressing

HeLa cells shown maximum intensity projection images (MIP). The inset indicates a necklace-like string of centromeres observed in a nucleolus of control cells. (G) ChlR1-depleted cells have fewer perinuclear centromeres (a) but more total centromeres (b) than control cells. Centromere numbers were counted in the images acquired by the standard microscopy. Centromeres locating within 1.2 μm of the nuclear envelope were counted as perinuclear centromeres in (a). Asterisks indicate statistical significance at $p<0.0001$ by unpaired Student's t-test. Bars are standard error of the mean (SEM). Images of (A) were taken by standard fluorescence microscopy. Images of (C), (E) and (F) were taken by confocal fluorescence microscopy. The scale bars indicate 10 μm.

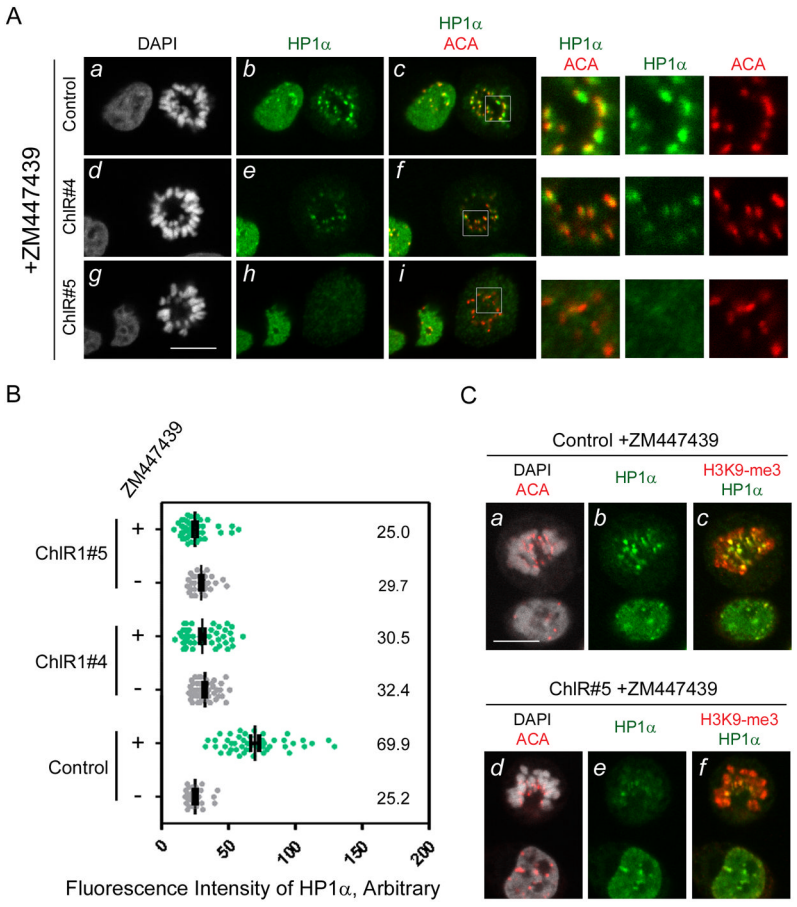


**Figure 2.**

Localization of HP1α to constitutive heterochromatin is impaired in ChlR-depleted HeLa cells. (A) Treatment of cells with an aurora kinase inhibitor, ZM447439, revealed a marked decrease in HP1α association with pericentric regions of mitotic chromosomes in the absence of ChlR. The bar indicates 10 μm. (B) Quantitative analyses of the fluorescence intensity of pericentric heterochromatin in mitotic cells. Pericentric HP1α signals in the images used in (A) was measured. The mean values are indicated with SEM. For each analysis, 2–3 mitotic cells carrying 27–48 pericentric regions were analyzed. (C) H3K9-me3 is retained in pericentric regions in ChlR-depleted cells. The bar indicates 10 μm.

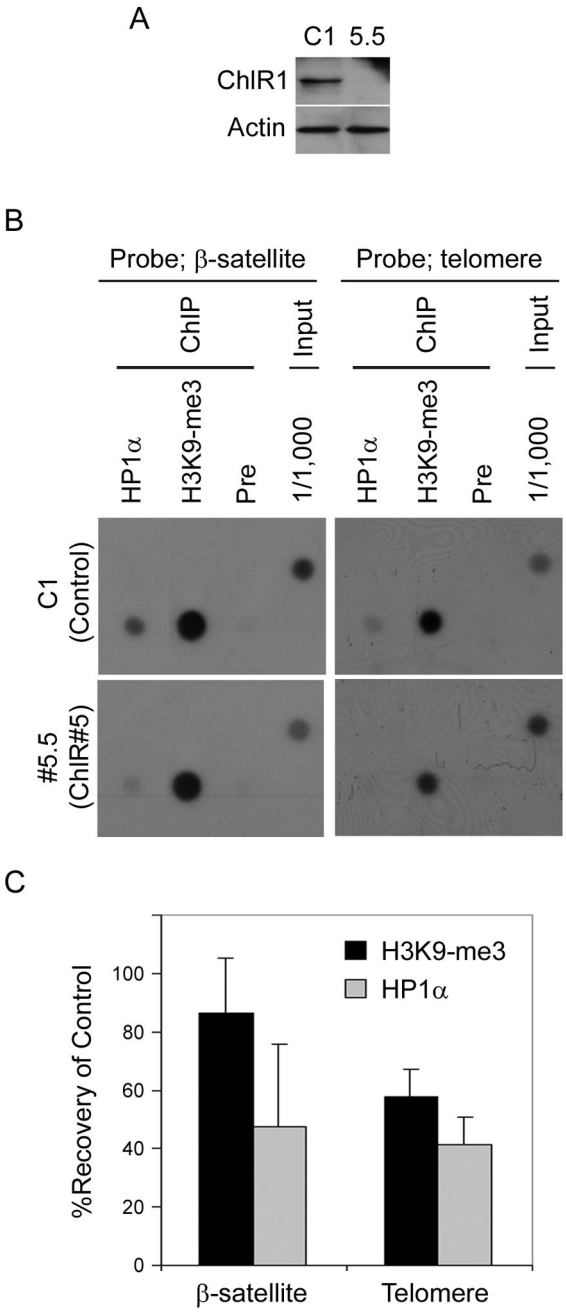


**Figure 3.**

Chromatin immunoprecipitation (ChIP) indicates decreased association of HP1α and H3K9-me3 in ChlR1-depleted cells. (A) Immunoblot showing a complete depletion of ChlR1 in a stable clone of ChlR1-shRNA expressing HeLa cells, which are used in (B). (B) Chromatin immunoprecipitation (ChIP) shows impaired binding of HP1α and H3K9-me3 in heterochromatin regions. (C) The graphs show the averages of 3 experiments. Bars indicate standard deviation (S.D.).

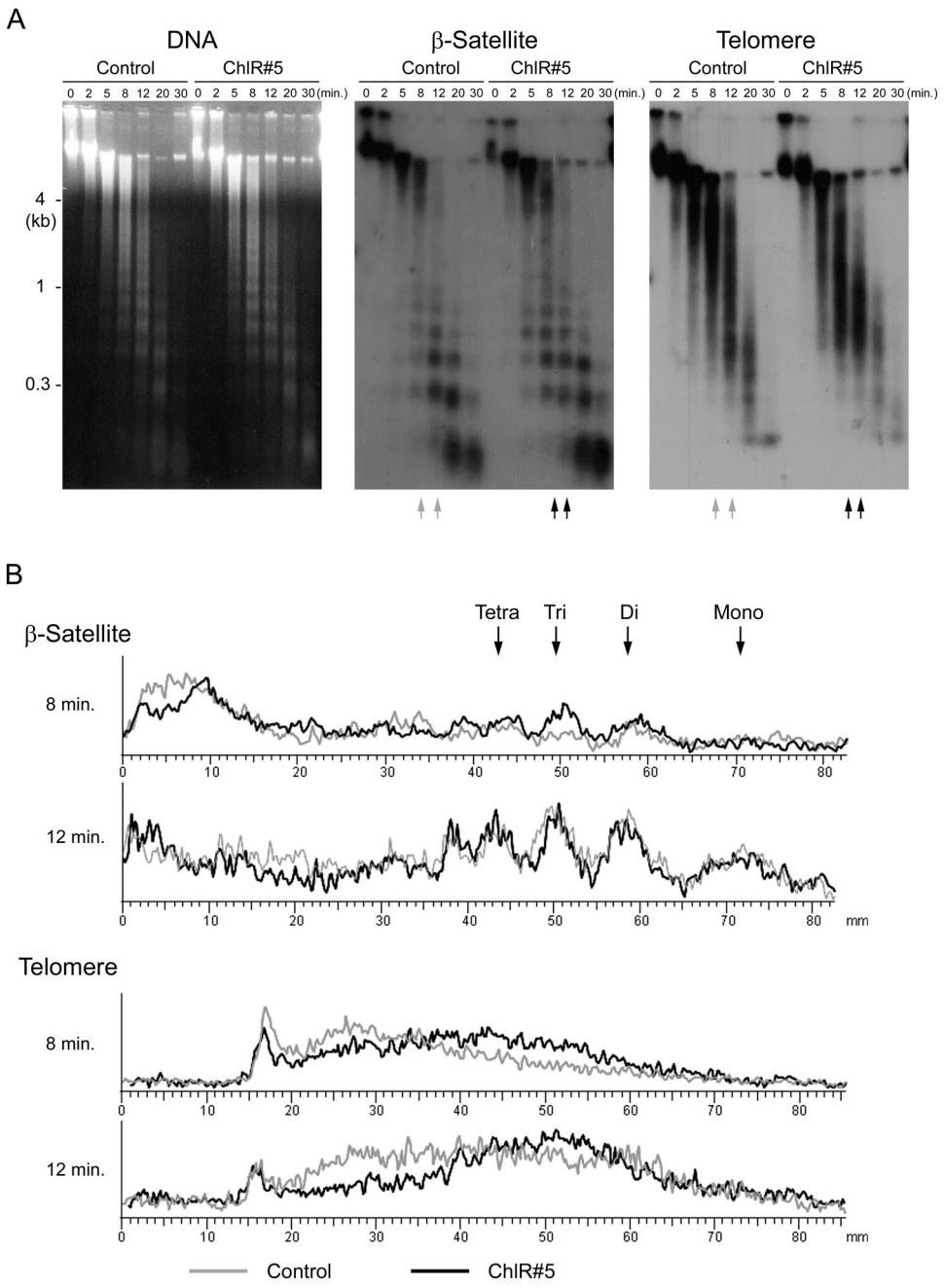


**Figure 4.**

ChlR-depleted cells have decreased chromatin density at telomeres. (A) Micrococcal nuclease (MNase) assay indicates a normal pattern of chromatin structure in β-satellite regions but sparse chromatin density in telomeres in ChlR-depleted cells. DNA of permeabilized cells was treated *in situ* with MNase for the indicated time and the chromatin was collected and separated by agarose gel electrophoresis. The DNAs were transferred to Nylon filter membrane, followed by hybridization with probes for human repetitive sequences. (B) Radioactivity along the lanes indicated by arrows in (A) acquired from the hybridization with β-satellite and telomere probes was measured by a phosphoimager and plotted. Positions of the oligonucleosomes are indicated at the top.

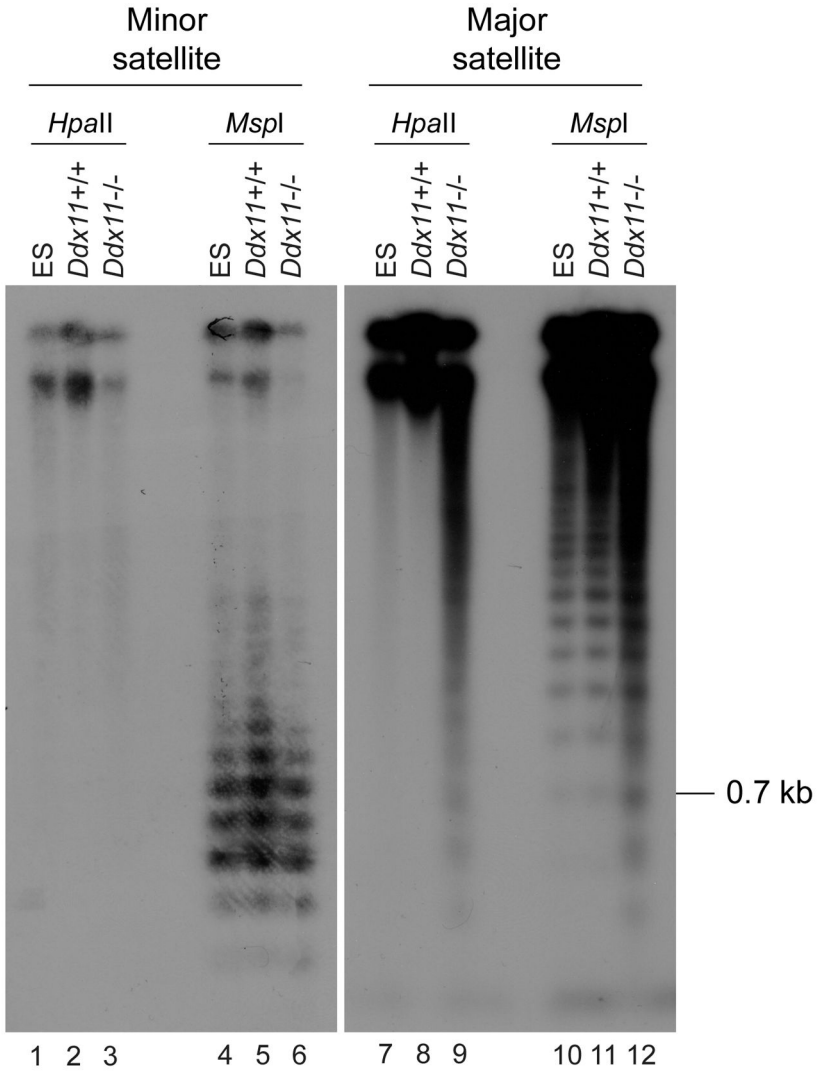


**Figure 5.**

*Ddx11*$^{-/-}$ embryos have impaired DNA methylation at pericentric repeats. DNAs isolated from *Ddx11*$^{+/+}$ ES cells, *Ddx11*$^{+/+}$ E9.5 embryos, and *Ddx11*$^{-/-}$ E9.5 embryos were digested with *Hpa*II or *Msp*I and analyzed by Southern hybridization using minor and major satellite probes.

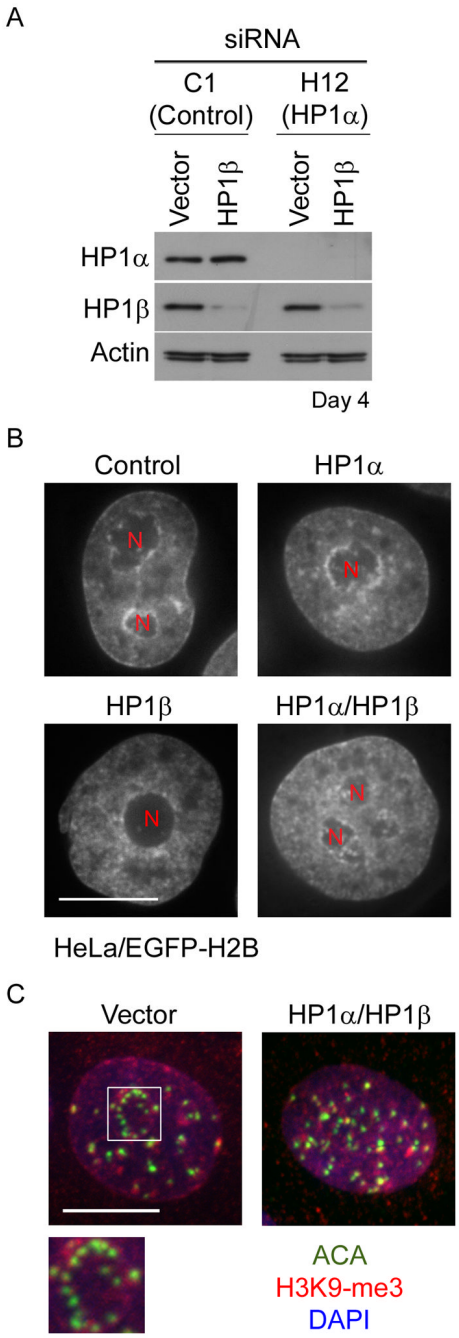


**Figure 6.**

HeLa cells depleted of both HP1α and HP1β exhibit morphological phenotypes similar to those found in the absence of ChlR. (A) Immunoblot showing depletion of HP1α and/or HP1β in HeLa cells. (B) HP1β- and HP1α/HP1β-depleted HeLa cells expressing EGFP-H2B show dispersed chromatin distribution. (C) HP1α/HP1β-depleted HeLa cells show disrupted centromere localization. Bars indicate 10 μm.